A well-defined moving steady states capturing Godunov-type scheme for Shallow-water model

Christophe Berthon, Meissa M'Baye, Minh H. Le, Diaraf Seck

A well-defined moving steady states capturing Godunov-type scheme for Shallow-water model

Christophe Berthon
Université de Nantes, CNRS UMR 6629, Laboratoire de Mathématiques Jean Leray, rue de la Houssinière, BP 92208, 44322 Nantes, France.
christophe.berthon@univ-nantes.fr

Meissa M'baye
Université de Nantes, CNRS UMR 6629, Laboratoire de Mathématiques Jean Leray, rue de la Houssinière, BP 92208, 44322 Nantes, France and Université Cheikh Anta Diop de Dakar (UCAD), Dakar, Sénégal.
meissa.mbaye@univ-nantes.fr

Minh Hoang Le
Laboratoire d'hydraulique Saint Venant (LHSV), 6 Quai Watier 78400 Chatou, France.
minh-hoang.le@enpc.fr

Diaraf Seck
Laboratoire de Mathématiques de la Décision et d'Analyse Numérique (LMDAN), FASEG, Université Cheikh Anta Diop, BP 16889 Dakar, Sénégal.
diaraf.seck@ucad.edu.sn

Key words : Hyperbolic conservation laws, Balance laws, Fully Well-balanced schemes, Godunov-type schemes, entropy inequalities.

Abstract

The present work concerns the derivation of a well-balanced scheme to approximate the weak solutions of the shallow-water model. Here, the numerical scheme exactly captures all the smooth steady solutions with non-vanishing velocities. To address such an issue, a Godunov-type scheme is adopted. A particular attention is paid on the derivation of the intermediate states within the approximate Riemann solver. Indeed, because of the moving steady states, the intermediate states may be ill-defined. Here, we introduce a suitable correction in order to get a fully well-defined finite volume scheme. In addition, the numerical method is established to be positive preserving and to satisfy a discrete entropy inequality up to small perturbations. Several numerical experiments, including wet/dry transition, illustrate the relevance of the designed scheme.

1 Introduction

The present works is devoted to the numerical approximation of the solutions of the well-known shallow-water system given as follows:

$$\begin{cases} \partial_t h + \partial_x hu = 0, & x \in \mathbb{R},\ t > 0, \\ \partial_t hu + \partial_x \left(hu^2 + g\dfrac{h^2}{2} \right) = -gh\partial_x z, \end{cases} \tag{1}$$

where $h(x,t) \geq 0$ stands for the water height and $u(x,t) \in \mathbb{R}$ denotes the water velocity. Here, $g > 0$ is the gravitational constant and $z(x)$ is a given smooth function to represent the bottom topography. For the sake of simplicity in the forthcoming notations, we set

$$w = \begin{pmatrix} h \\ hu \end{pmatrix}, \quad f(w) = \begin{pmatrix} hu \\ hu^2 + g\dfrac{h^2}{2} \end{pmatrix} \quad \text{and} \quad S(w,z) = \begin{pmatrix} 0 \\ -gh\partial_x z \end{pmatrix}.$$

In addition, we introduce $\Omega \subset \mathbb{R}^2$ the set of physical admissible states given by

$$\Omega = \{w \in \mathbb{R}^2;\ h > 0,\ u \in \mathbb{R}\}.$$

At this level, we do not consider the dry areas and we have imposed $h > 0$. However, the derived scheme will be seen relevant to deal with wet/dry transitions. Since the first-order extracted system is knows to be hyperbolic, in a finite time, the solution may contain discontinuities governed by the Rankine-Hugoniot conditions [14,27,28]. In order to rule out nonphysical solutions, the system (1) must be endowed with an entropy inequality defined by

$$\partial_t \eta(w) + \partial_x G(w) \leq -ghu\partial_x z, \tag{2}$$

where both entropy function $\eta : \Omega \to \mathbb{R}$ and entropy flux function $G : \Omega \to \mathbb{R}$ are given by

$$\eta(w) = h\frac{u^2}{2} + g\frac{h^2}{2} \qquad \text{and} \qquad G(w) = \left(\frac{u^2}{2} + gh \right) hu. \tag{3}$$

Now, considering the numerical approximation of the solution of the system (1), after the pioneer works by Bermudez [2] and Greenberg-LeRoux [18] (for instance, see also Gosse [16] or Jin [21]), the steady solutions must be accurately approximate to ensure the relevance of the designed scheme. These solutions of particular interest are governed by the following system:

$$\begin{cases} \partial_x (hu) = 0, \\ \partial_x \left(hu^2 + g\dfrac{h^2}{2} \right) = -gh\partial_x z. \end{cases} \tag{4}$$

After direct computations, the smooth steady solutions are defined by

$$\begin{cases} \partial_x (hu) = 0, \\ \partial_x \left(\dfrac{u^2}{2} + g(h+z) \right) = 0. \end{cases}$$

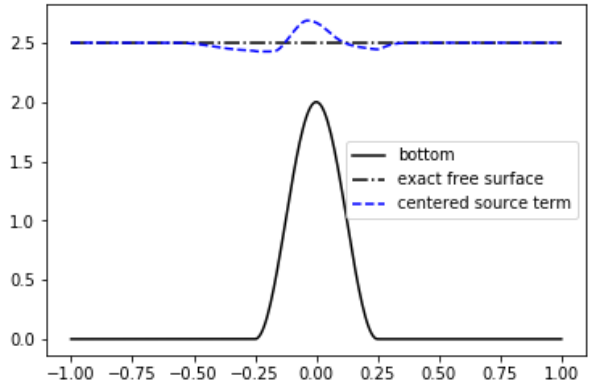

Figure 1: Numerical approximation of the lake at rest obtained by adopting an HLL first-order scheme [20] supplemented with a centred discretization of the source term.

As a consequence, for any given constant pair $(Q, B) \in \mathbb{R}^2$, the smooth steady solutions are characterized by the two following relations:

$$\begin{cases} hu = Q, \\ \dfrac{u^2}{2} + g(h+z) = B. \end{cases} \tag{5}$$

For the sake of simplicity in the forthcoming developments, we set

$$\mathcal{B}(w, z) = \frac{u^2}{2} + g(h+z). \tag{6}$$

During the two last decades, numerous works are devoted to the derivation of numerical schemes to approximate the weak solutions of (1) and able to accurately capture the steady solutions. Indeed, after [2, 17–19], if steady solutions are not correctly captured, the approximation may involve huge errors for large time (see Figure 1 for an illustration).

Since (5) turns out to be nonlinear, several works only consider the lake at rest steady states defined by $u = 0$ and a constant free surface $h + z$. For instance the reader is referred to the well-known hydrostatic reconstruction introduce by Audusse and al. [1] (see also [6]). Such an easy technique has been adopted in lot of situations and the preservation of the lake at rest is now very usual to develop well-balanced scheme (see [5,7,9,10] for a non exhaustive list of references). Since (5) may admit one, two or three solutions according to the choice of the pair $(Q, B) \in \mathbb{R} \times \mathbb{R}^+$, it is clear that the derivation of a scheme able to capture all smooth steady solutions is a very challenging. In [16], the nonlinear system (5) is solved at each interface to get a fully well-balanced scheme able to exactly capture all the smooth steady solutions (moving and non moving). Next, in [8], the authors proposed a suitable extension of the hydrostatic reconstruction in order to deal with moving steady solutions. Unfortunately, this generalized hydrostatic reconstruction does not preserve the water height non negative. Several works by Xing [24, 30, 31] (see also [25, 26]) proposed relevant extensions of the high order discontinuous Galerkin method to preserve all the steady states solutions of (5).

More recently, in [3], a Godunov-type scheme is derived in order to introduce the source term within the approximate Riemann solver. They got a positive and entropy preserving scheme which exactly capture all the smooth steady solutions. Unfortunately, once again, a strongly non linear equation must be solved at each interface.

Next, in [22,23], a relevant linearization of the Godunov-type scheme is designed to get a positive preserving fully well-balanced scheme. From now on, we underline that this numerical technique exactly capture all the steady solutions without solving (5), which make very attractive such a scheme. However, the obtained topography source term discretization involves some difficulties. Indeed, in [22, 23], the source term is approximated at each interface as follows:

$$(h\partial_x z)^n_{i+1/2} = \frac{h_i^n h_{i+1}^n}{(h_i^n + h_{i+1}^n)/2} \times \frac{z_{i+1} - z_i}{\Delta x} + \frac{1}{2(h_i^n + h_{i+1}^n)} \times \frac{[h]^3_{i+1/2}}{\Delta x}, \tag{7}$$

where

$$[h]_{i+1/2} = \begin{cases} h_{i+1}^n - h_i^n & \text{if} \quad |h_{i+1}^n - h_i^n| \leq C\Delta x, \\ C\Delta x & \text{otherwise.} \end{cases} \tag{8}$$

Here, the definition of the constant C remains open. Moreover, we remark that, with a flat topography, the source term is given by $\mathcal{O}(\Delta x^2)$ instead of zero. In addition, the adopted linearization introduces a perturbation within the definition of the numerical flux function given by

$$\frac{(h\partial_x z)^n_{i+1/2}}{g\frac{h_i^n + h_{i+1}^n}{2} - \frac{(q_i^2 + q_{i+1}^2)/2}{h_i^n h_{i+1}^n}} \Delta x. \tag{9}$$

Such a perturbation is necessary to recover the exact capture of the moving steady states. But we note that this needed above perturbation may be undefined as soon as we have

$$g\frac{h_i^n + h_{i+1}^n}{2} = \frac{(q_i^n)^2 + (q_{i+1}^n)^2}{2h_i^n h_{i+1}^n}. \tag{10}$$

This failure is underlined in [22, 23], but the authors claimed that the equality (10) never holds during the numerical experiments. However, it seems that this lack of consistency may produce numerical errors as illustrated in Figure 2.

The objective of the present paper is twofold. First, we propose a new source term discretization which is naturally consistent without involving some cutoff technique as introduce in (7)-(8). Next, the fully well-balanced perturbation (9) is improved in order to get a well-defined numerical method. In addition, the resulting fully well-balanced scheme must be water positive preserving and entropy preserving in a sense to be prescribed.

To address such an issue, the paper is organized as follows. In the next section, we design the Godunov-type scheme with source term. Such a scheme comes form a suitable definition of the approximate Riemann solver. After [3, 22, 23], the mains novelty here stays in the introduction of the source term in the definition of the approximate Riemann solver. The next section, is devoted to design a relevant approximation of the source term to be put within the approximate Riemann solver.

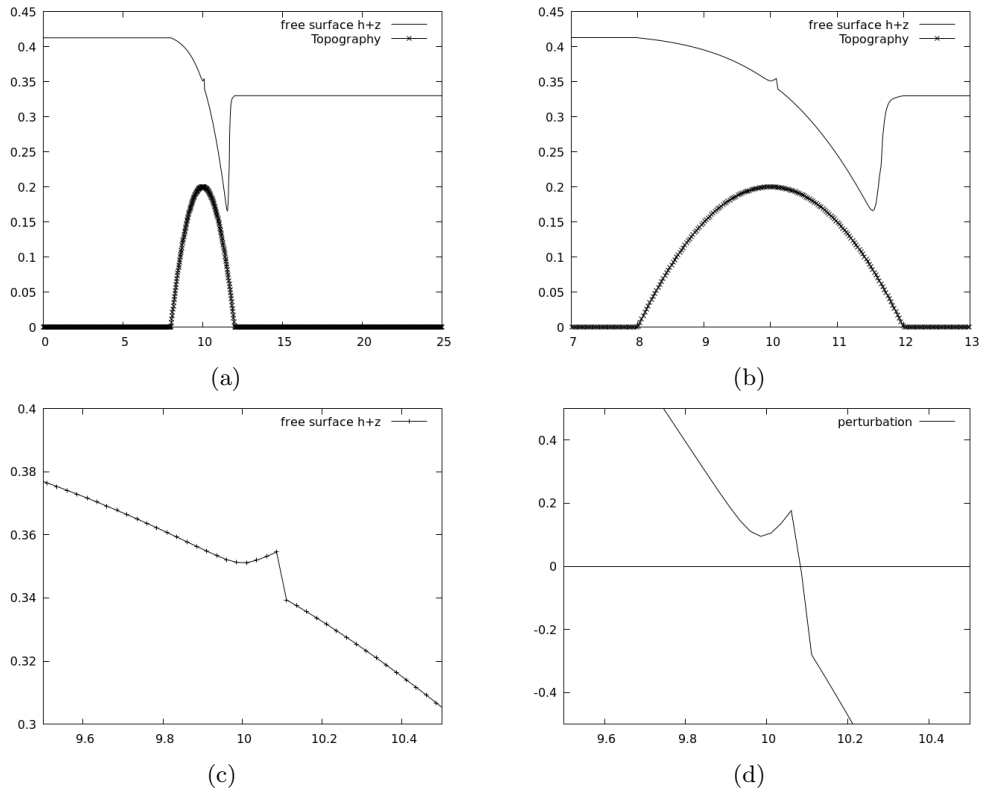

Figure 2: Figure (a) displays the free surface for a transcritical flow with shock test case obtained by the scheme introduced in [22, 23]. In (b), we present a zoom of the spurious perturbation of the water height produced by the ill-posed quantity $\mathcal{P} = g\frac{h_i^n+h_{i+1}^n}{2} - \frac{(q_i^n)^2+(q_{i+1}^n)^2}{2h_i^n h_{i+1}^n}$. In order to illustrate the failure of this method, in (c) and (d), we respectively present the behavior of the water height and ill-posed quantity $\mathcal{P}$. We remark that $\mathcal{P}$ vanishes and produces the spurious perturbation.

Here, we impose to the source term approximation to be fully consistent in order to avoid some cutoff technique. The fourth section concerns the complete derivation of the approximate Riemann solver. A suitable improvement is adopted to get a well defined fully well-balanced scheme. Next, in Section 5, we exhibit the main properties satisfied by the derived scheme. In the last section, several numerical approximations, including wet/dry transition, illustrate the relevance of the proposed scheme.

2 Godunov-type schemes for shallow-water with source term

To approximate the solution of (1), we first introduce a space discretization made of cells $(x_{i-1/2}, x_{i+1/2})$ with a constant size Δx. Then, we have $x_{i+1/2} = x_{i-1/2} + \Delta x$ for all $i \in \mathbb{Z}$ and we denote $x_i = x_{i-1/2} + \Delta x/2$ the cell center. Considering the time discretization, we set $t^{n+1} = t^n + \Delta t$ where the time increments Δt must be restricted according to a CFL-like condition.

At time t^n, we assume known a constant piecewise approximation of the solution of (1) as follows:

$$w_\Delta^n(x, t = 0) = w_i^n \qquad \text{if } x \in (x_{i-1/2}, x_{i+1/2}).$$

We research for an updated approximation of the solution at time $t^{n+1} = t^n + \Delta t$. To address such an issue, after [15, 20, 28], the updated state w_i^{n+1} is given by

$$w_i^{n+1} = \frac{1}{\Delta x} \int_{x_{i-1/2}}^{x_{i+1/2}} w_\Delta^n(x, \Delta t)\, dx, \tag{11}$$

where $w_\Delta^n(x,t)$ stands for the juxtaposition of non-interacting approximate Riemann solvers stated at each interface $x_{i+1/2}$ as follows:

$$w_\Delta^n(x,t) = \widetilde{w}_{\mathcal{R}}\left(\frac{x - x_{i+1/2}}{t}; w_i^n, w_{i+1}^n, z_i, z_{i+1}\right) \quad \text{if} \quad (x,t) \in (x_i, x_{i+1}) \times (0, \Delta t).$$

Here, $\widetilde{w}_{\mathcal{R}}\left(\frac{x}{t}; w_L, w_R, z_L, z_R\right)$ denotes a suitable approximation of Riemann solution of (1) associated with the initial data

$$(w,z)(x, t = 0) = \begin{cases} (w_L, z_L) & \text{if } x < 0, \\ (w_R, z_R) & \text{if } x > 0. \end{cases} \tag{12}$$

According to [20], the approximate Riemann solver has to satisfy the following integral consistency condition:

$$\begin{aligned} \frac{1}{\Delta x} \int_{-\Delta x/2}^{\Delta x/2} \widetilde{w}_{\mathcal{R}}(\frac{x}{t}; w_L, w_R, z_L, z_R)\, dx = \\ \frac{1}{\Delta x} \int_{-\Delta x/2}^{\Delta x/2} w_{\mathcal{R}}(\frac{x}{t}; w_L, w_R, z_L, z_R)\, dx, \end{aligned} \tag{13}$$

where $w_{\mathcal{R}}(\frac{x}{t}; w_L, w_R, z_L, z_R)$ is nothing but the exact solution of the Riemann problem for (1) associated with the initial data (12). Now, since the system (1) under consideration contains a source term, the average of the exact Riemann solution is not reachable. Indeed, as long as Δt is small enough such that

$$w_{\mathcal{R}}\left(\frac{-\Delta x/2}{\Delta t}; w_L, w_R, z_L, z_R\right) = w_L \quad \text{and} \quad w_{\mathcal{R}}\left(\frac{\Delta x/2}{\Delta t}; w_L, w_R, z_L, z_R\right) = w_R,$$

the integration of (1) over the domain $(-\Delta x/2, \Delta x/2)\times(0, \Delta t)$, after straightforward computation, reads

$$\begin{aligned}\frac{1}{\Delta x}\int_{-\Delta x/2}^{\Delta x/2} w_{\mathcal{R}}(\frac{x}{t}; w_L, w_R, z_L, z_R)\, dx = \frac{1}{2}(w_L + w_R) - \frac{\Delta t}{\Delta x}(f(w_R) - f(w_L)) \\ - \frac{g}{\Delta x}\int_0^{\Delta t}\int_{-\Delta x/2}^{\Delta x/2} \widetilde{(h\partial z)}_{\mathcal{R}}(\frac{x}{\Delta t}, w_L, w_R, z_L, z_R)\, dx.\end{aligned} \tag{14}$$

Because of the source term integral, which must be defined in a prescribed sense, the expected average of the exact Riemann solution is, a priori, not correctly defined. As a consequence, we suggest to introduce $\bar{S}_{LR}$ to approximate this integral (for instance, see [11,12]). Hence, we impose the approximate Riemann solver to satisfy, instead of (13), the following approximated consistency condition:

$$\begin{aligned}\frac{1}{\Delta x}\int_{-\Delta x/2}^{\Delta x/2} \widetilde{w}_{\mathcal{R}}(\frac{x}{t}; w_L, w_R, z_L, z_R)\, dx = \\ \frac{1}{2}(w_L + w_R) - \frac{\Delta t}{\Delta x}(f(w_R) - f(w_L)) + \Delta t \bar{S}_{LR},\end{aligned} \tag{15}$$

where $\bar{S}_{LR} = \bar{S}_{LR}(w_L, w_R, z_L, z_R)$ must be defined according to a consistent discretization of $(0, -gh\partial_x z)^T$. Now equipped with the approximate Riemann solver $\widetilde{w}_{\mathcal{R}}(\frac{x}{\Delta t}; w_L, w_R, z_L, z_R)$, the updated state w_i^{n+1}, can be reformulate in a standard finite volume formulation. Indeed, from (11) we easily get

$$\begin{aligned}w_i^{n+1} = \frac{1}{\Delta x}\int_{x_{i-1/2}}^{x_i} \tilde{w}_{\mathcal{R}}\left(\frac{x - x_{i-1/2}}{\Delta t}; w_{i-1}^n, w_i^n, z_{i-1}, z_i\right)\, dx + \\ \frac{1}{\Delta x}\int_{x_i}^{x_{i+1/2}} \tilde{w}_{\mathcal{R}}\left(\frac{x - x_{i+1/2}}{\Delta t}; w_i^n, w_{i+1}^n, z_i, z_{i+1}\right)\, dx.\end{aligned}$$

According to the interface location $x_{i+1/2}$, we adopt a change of variable, given by $x \to x - x_{i+1/2}$, to obtain

$$\begin{aligned}\frac{1}{\Delta x}\int_{x_i}^{x_{i+1/2}} \tilde{w}_{\mathcal{R}}\left(\frac{x - x_{i+1/2}}{\Delta t}; w_i^n, w_{i+1}^n, z_i, z_{i+1}\right)\, dx = \\ \frac{1}{\Delta x}\int_{-\Delta x/2}^{0} \tilde{w}_{\mathcal{R}}\left(\frac{x}{\Delta t}; w_i^n, w_{i+1}^n, z_i, z_{i+1}\right)\, dx \\ \frac{1}{\Delta x}\int_{x_{i+1/2}}^{x_{i+1}} \tilde{w}_{\mathcal{R}}\left(\frac{x - x_{i+1/2}}{\Delta t}; w_i^n, w_{i+1}^n, z_i, z_{i+1}\right)\, dx = \\ \frac{1}{\Delta x}\int_{0}^{\Delta x/2} \tilde{w}_{\mathcal{R}}\left(\frac{x}{\Delta t}; w_i^n, w_{i+1}^n, z_i, z_{i+1}\right)\, dx.\end{aligned}$$

For the sake of simplicity in the notations, we set

$$I^-_{i+1/2} = \frac{1}{\Delta x}\int_{-\Delta x/2}^{0} \widetilde{w}_{\mathcal{R}}\left(\frac{x}{\Delta t}; w_i^n, w_{i+1}^n, z_i, z_{i+1}\right)\, dx, \tag{16}$$

$$I^+_{i+1/2} = \frac{1}{\Delta x}\int_{0}^{\Delta x/2} \widetilde{w}_{\mathcal{R}}\left(\frac{x}{\Delta t}; w_i^n, w_{i+1}^n, z_i, z_{i+1}\right)\, dx, \tag{17}$$

so that the updated state w_i^{n+1} immediately rewrites as follows:

$$\begin{aligned} w_i^{n+1} &= I^+_{i-1/2} + I^-_{i+1/2}, \\ &= \frac{1}{2}\left(I^-_{i-1/2} + I^+_{i-1/2}\right) + \frac{1}{2}\left(I^-_{i+1/2} + I^+_{i+1/2}\right) \\ &\qquad + \frac{1}{2}\left(I^+_{i-1/2} - I^-_{i-1/2}\right) + \frac{1}{2}\left(I^-_{i+1/2} - I^+_{i+1/2}\right). \end{aligned}$$

Since, for all $i \in \mathbb{Z}$

$$\frac{1}{2}\left(I^-_{i+1/2} + I^+_{i+1/2}\right) = \frac{1}{\Delta x}\int_{-\Delta x/2}^{\Delta x/2} \tilde{w}_{\mathcal{R}}\left(\frac{x}{\Delta t}; w_i^n, w_{i+1}^n, z_i, z_{i+1}\right)\, dx,$$

arguing the consistency condition (15), we obtain

$$\begin{aligned} w_i^{n+1} \;=\; & w_i^n - \frac{\Delta t}{\Delta x}\left(f_\Delta(w_i^n, w_{i+1}^n, z_i, z_{i+1}) - f_\Delta(w_{i-1}^n, w_i^n, z_{i-1}, z_i)\right) \\ & + \frac{\Delta t}{2}\left(\bar{S}_{i+1/2} + \bar{S}_{i-1/2}\right), \end{aligned} \tag{18}$$

with the numerical flux function given by

$$f_\Delta(w_R, w_L, z_L, z_R) = \frac{1}{2}(f(w_R) + f(w_L)) - \frac{\Delta x}{4\Delta t}(w_R - w_L) + \frac{\Delta x}{2\Delta t}\left(I^+_{LR} - I^-_{LR}\right),$$

where

$$I^+_{LR} = \frac{1}{\Delta x}\int_{0}^{\Delta x/2} \widetilde{w}_{\mathcal{R}}\left(\frac{x}{\Delta t}; w_L, w_R, z_L, z_R\right) dx,$$

$$I^-_{LR} = \frac{1}{\Delta x}\int_{-\Delta x/2}^{0} \widetilde{w}_{\mathcal{R}}\left(\frac{x}{\Delta t}; w_L, w_R, z_L, z_R\right) dx.$$

Concerning the source term discretization, with clear notations, we have

$$\bar{S}_{i+1/2} := \bar{S}_{LR}(w_i^n, w_{i+1}^n, z_i, z_{i+1}),$$

where $\bar{S}_{LR}$ is introduce in (15). The presentation of the Godunov-type scheme with source term is then achieved. Now, the full scheme derivation will be completed as soon as the approximate Riemann solver $\widetilde{w}_{\mathcal{R}}(x/\Delta t; w_L, w_R, z_L, z_R)$ and the source term approximation $\bar{S}_{LR}(w_L, w_R, z_L, z_R)$ are characterized.

3 Discretization of the source term

In this section, the local approximation of the source term $\bar{S}_{LR}(w_L, w_R, z_L, z_R)$, stated at each interface, is defined in order to preserve the stationary solutions. First, according to (5), a locally steady solution is defined as follows:

$$h_L u_L = h_R u_R, \qquad and \qquad \mathcal{B}(w_L, z_L) = \mathcal{B}(w_R, z_R), \tag{19}$$

where $\mathcal{B}(w, z)$ is given by (6). As a consequence, $\bar{S}_{LR}$ must be fixed such that $\widetilde{w}_{\mathcal{R}}(x/\Delta t; w_L, w_R, z_L, z_R)$ remains stationary; namely

$$\widetilde{w}_{\mathcal{R}}(x/\Delta t, w_L, w_R, z_L, z_R) = \begin{cases} w_L & \text{if} \quad x < 0, \\ w_R & \text{if} \quad x > 0. \end{cases} \tag{20}$$

as soon as (w_L, w_R, z_L, z_R) satisfies (19). Now, let us underline that the integral consistency condition (15), for smooth steady solution in the form (20), rewrites as follows:

$$\Delta x \bar{S}_{LR} = f(w_R) - f(w_L).$$

Since (w_L, w_R, z_L, z_R) are given according (19), with $\bar{S}_{LR} = (\bar{S}^h_{LR}, \bar{S}^q_{LR})^T$, we get

$$\Delta x \bar{S}^h_{LR} = 0,$$

$$\Delta x \bar{S}^q_{LR} = (h_R u_R^2 + g\frac{h_R^2}{2}) - (h_L u_L^2 + g\frac{h_L^2}{2}). \tag{21}$$

Since the evolution equation of the water height does not contain source term, we fix $\bar{S}^h_{LR} = 0$. We focus our attention on $\bar{S}^q_{LR}$ and we have to design this quantity in order to be consistent with the topography source term $-gh\partial_x z$ and such that (21) holds as soon as (w_L, w_R, z_L, z_R) defines a local steady solution (19). To address such an issue, we now state a necessary condition to be satisfied by $\bar{S}^q_{LR}$.

Lemma 3.1 Let us introduce

$$\bar{F}_r^2 = \frac{q_0^2 \bar{h}}{g h_L^2 h_R^2}, \qquad \text{where } \bar{h} = \frac{1}{2}(h_L + h_R) \text{ and } q_0 = h_L u_L = h_R u_R, \tag{22}$$

an approximation of the well-known Froude number. As soon as $\bar{F}_r \neq 1$ and (w_L, w_R, z_L, z_R) are steady states according to (19), the identity (21) reformulates as follows:

$$\Delta x \bar{S}^q_{LR} = -g\bar{h}(z_R - z_L) + \frac{q_0^2}{4h_L^2 h_R^2} \times \frac{(h_R - h_L)(z_R - z_L)^2}{(1 - \bar{F}_r^2)^2}. \tag{23}$$

From now on, we remark that (23) immediately gives a consistent definition of $\bar{S}^q_{LR}$. Indeed, for smooth enough topography function, we have

$$\lim_{\Delta x \to 0} \frac{(z_R - z_L)^2}{\Delta x} = 0,$$

to ensure that $\bar{S}^q_{LR}$ is consistent with $-gh\partial_x z$. However, this relevant definition of $\bar{S}^q_{LR}$ must be improved in order to deal with $\bar{F}_r = 1$. Now, we establish the above lemma.

Proof With $q_0 = h_L u_L = h_R u_R$, the relation (21) easily rewrites

$$\Delta x \bar{S}^q_{LR} = q_0 \left(\frac{1}{h_R} - \frac{1}{h_L} \right) + g\bar{h}(h_R - h_L),$$

to get

$$\Delta x \bar{S}^q_{LR} = \left(g\bar{h} - \frac{q_0^2}{h_L h_R} \right) (h_R - h_L). \tag{24}$$

Now, since we have $\mathcal{B}(w_L, z_L) = \mathcal{B}(w_L, z_L)$ with $\mathcal{B}(w, z)$ given by (6), we have

$$\frac{q_0^2}{2h_L^2} + g(h_L + z_L) = \frac{q_0^2}{2h_R^2} + g(h_R + z_R),$$

to obtain

$$(h_R - h_L) + (z_R - z_L) = \frac{q_0^2}{2g} \times \frac{h_R^2 - h_L^2}{h_L^2 h_R^2}.$$

We introduce $\bar{F}_r$, defined by (22), to write the above relation as follows:

$$h_R - h_L = -\frac{z_R - z_L}{1 - \bar{F}_r^2}. \tag{25}$$

Next, we plug the above water height jump into (24) to have

$$\Delta x \bar{S}_{LR} = -g\bar{h} \times \frac{\left(1 - \frac{q_0^2}{g h_L h_R \bar{h}}\right)}{\left(1 - \bar{F}_r^2\right)} \times (z_R - z_L), \tag{26}$$

which rewrites as follows:

$$\Delta x \bar{S}_{LR} = -g\bar{h}(z_R - z_L) - \frac{q_0^2}{4h_L^2 h_R^2} \times \frac{(h_L - h_R)^2}{1 - \bar{F}_r^2} \Delta z. \tag{27}$$

The expected identity (23) is obtained by introducing (25) into (27). The proof is then completed. □

In order to propose a suitable correction within (23) to get a well-defined discretization of the source term, we exhibit the behavior of (23) in the limit of $\bar{F}_r$ to 1.

Lemma 3.2 Let us consider (w_L, w_R, z_R, z_L) according to (19) so that $\bar{S}^q_{LR}$ is given by (23). Then we have

$$\lim_{\bar{F}_r \to 1} \bar{S}^q_{LR} = \mathcal{O}(\Delta x^2).$$

Proof Since (w_L, w_R, z_L, z_R) is given according (19), then the relation (25) holds and we easily reformulate (23) as follows:

$$\Delta x \bar{S}^q_{LR} = g\bar{h}(h_R - h_L)(1 - \bar{F}_r^2) + \frac{g\bar{F}_r^2}{4\bar{h}}(h_R - h_L)^3,$$

to immediately obtain the following limit

$$\lim_{\bar{F}_r^2 \to 1} \bar{S}_{LR}^q = \frac{g}{4\bar{h}} \frac{(h_R - h_L)^3}{\Delta x}. \tag{28}$$

First, as soon as the water height is a smooth solution, we have $h_R - h_L = \mathcal{O}(\Delta x)$ and the proof is achieved. Next let us show that, in the limit of $\bar{F}_r$ to 1, necessarily the approximated water height is smooth and then $h_R - h_L = \mathcal{O}(\Delta x)$. Indeed, let us assume w_L and w_R be connected by a stationary shock solution. Because of the Rankine-Hugoniot relations (see [27]), since the shock velocity is equal to 0, we have

$$\begin{aligned} &q_L = q_R = q_0, \\ &\left(\frac{q_R^2}{h_R} + g\frac{h_R^2}{2}\right) - \left(\frac{q_L^2}{h_L} + g\frac{h_L^2}{2}\right) = 0, \end{aligned}$$

so that we obtain

$$(h_R - h_L) g\bar{h} \left(1 - \frac{q_0^2}{g\bar{h} h_L h_R}\right) = 0, \tag{29}$$

where $\bar{h}$ is defined by (22). With $h_L \neq h_R$, from (29), it comes $\frac{q_0^2}{g\bar{h} h_L h_R} = 1$. In the limit of Fr to 1, with $\bar{F}_r$ given by (22), we get

$$\frac{q_0^2}{g\bar{h} h_L h_R} = \frac{q_0^2 \bar{h}}{g h_L^2 h_R^2},$$

to obtain $h_L = h_R$ in contradiction with $h_L \neq h_R$. As a consequence, in the limit of $\bar{F}_r$ to 1, we always have $h_R - h_L = \mathcal{O}(\Delta x)$. The proof is then completed. □

In fact, the above result states that the discretization (23) is well-defined for all values of $\bar{F}_r$ as long as the local equilibrium condition (19) is satisfied. As a consequence, (23) must be improved in order to be well-defined for all values of $\bar{F}_r$ with left and right states not verifying a local steady solution (19). We now suggest an improvement in order to get a formula well-defined for all values of $\bar{F}_r$. In the present work, we propose the following discretization of the topography source term

$$\Delta x \bar{S}_{LR}^q = -g\bar{h}(z_R - z_L) + \frac{\overline{q^2}}{4h_L^2 h_R^2} \times \frac{(h_R - h_L)(z_R - z_L)^2}{(1 - \bar{F}_r^2)^2 + \varepsilon_{LR} \Delta x^k}, \tag{30}$$

where $k > 0$ is a parameter to be fixed and

$$\overline{q^2} = |q_L q_R|, \qquad \varepsilon_{LR} = \sqrt{|\mathcal{B}(w_R, z_R) - \mathcal{B}(w_L, z_L)| + |q_R - q_L|}. \tag{31}$$

From now on, we note that $\varepsilon_{LR} = 0$ if and only if (w_L, w_R, z_L, z_R) define a local steady solution according to (19). As a consequence, the suggested discretization (30) satisfy the necessary condition (23) for local steady solution. Moreover, the discretization (30) is well-defined for all values of $\bar{F}_r$. Indeed, as long as, the local equilibrium, given by (19), is satisfied, arguing Lemma 3.2 the source term discretization is well-defined as expected. Next, for non-steady states, since $(1 - \bar{F}_r^2)^2 + \varepsilon_{LR} \Delta x^k \neq 0$, once again (30) is well-defined for all values of $\bar{F}_r$. Of course, since the correction is given by $\varepsilon_{LR} \Delta x^k$, the consistency property of $\bar{S}_{LR}^q$ is

preserved. Moreover, according to the continuous extension argument given Lemma 3.2, we impose $\bar{S}^q_{LR} = 0$ if we have simultaneously $\bar{F}_r = 1$ and $\varepsilon_{LR} = 0$.

Now, concerning the value of $k > 0$, let us underline a specific behavior of $\bar{S}^q_{LR}$ with $\bar{F}_r = 1$ but far away from local equilibrium. Indeed, enforcing $\bar{F}_r = 1$, we have

$$\bar{S}^q_{LR} = -g\bar{h}\frac{(z_R - z_L)}{\Delta x} + \frac{\overline{q^2}}{4h_L^2 h_R^2} \times \frac{(h_R - h_L)(z_R - z_L)^2}{\varepsilon_{LR}} \Delta x^{-1-k},$$

since the topography function is smooth, we have $z_R - z_L = \mathcal{O}(\Delta x)$ so that

$$\bar{S}^q_{LR} = -g\bar{h}\frac{(z_R - z_L)}{\Delta x} + \frac{(h_R - h_L)}{\varepsilon_{LR}} \mathcal{O}(\Delta x^{1-k}).$$

Next, we have $\varepsilon_{LR} = \mathcal{O}(\Delta x^{1/2})$ with smooth enough solutions. Then we obtain

$$\bar{S}^q_{LR} = -g\bar{h}\frac{(z_R - z_L)}{\Delta x} + \mathcal{O}(\Delta x^{\frac{3}{2}-k}).$$

As a consequence, we fix $k = \frac{1}{2}$.

4 Approximate Riemann solver

To complete the characterisation of the numerical scheme (18), we now have to define a suitable approximate Riemann solver $\widetilde{w}_{\mathcal{R}}(x/t; w_L, w_R, z_L, z_R)$ according to the integral consistency condition (15) where the source term approximation $\bar{S}_{LR} = (0, \bar{S}^q_{LR})^T$ is defined by (30). In the present work, we adopt an approximate Riemann solver made of two intermediate constant states, w^*_L and w^*_R, as follows:

$$w_{\mathcal{R}}(x/t; v_L, v_R) = \begin{cases} w_L & \text{if } \frac{x}{t} < \lambda_L, \\ w^*_L & \text{if } \lambda_L < \frac{x}{t} < 0, \\ w^*_R & \text{if } 0 < \frac{x}{t} < \lambda_R, \\ w_R & \text{if } \frac{x}{t} > \lambda_R, \end{cases} \tag{32}$$

where $\lambda_L < 0$ and $\lambda_R > 0$ denote the discontinuity propagation speed. As usual (see [20, 29]), we impose

$$\lambda_L \leq \min(-|u_L| - \sqrt{gh_L}, -|u_R| - \sqrt{gh_R}),$$
$$\lambda_R \geq \max(|u_L| + \sqrt{gh_L}, |u_R| + \sqrt{gh_R}),$$

so that the cone defined by $\lambda_L \leq \frac{x}{t} \leq \lambda_R$ contains the exact cone coming from the exact Riemann solution associated with the initial data (12). Now, the integral consistency condition (15) reads as follows:

$$\lambda_L(h^*_L - h_L) + \lambda_R(h_R - h^*_R) = q_R - q_L, \tag{33}$$
$$\lambda_L(q^*_L - q_L) + \lambda_R(q_R - q^*_R) = \left(h_R u_R^2 + \frac{1}{2}gh_R^2\right) - \left(h_L u_L^2 + \frac{1}{2}gh_L^2\right) + \Delta x \bar{S}^q_{LR}. \tag{34}$$

For the sake of simplicity in the notations, let us introduce (see [20])

$$h^{HLL} = \frac{\lambda_R h_R - \lambda_L h_L}{\lambda_R - \lambda_L} - \frac{q_R - q_L}{\lambda_R - \lambda_L}, \tag{35}$$

$$q^{HLL} = \frac{\lambda_R q_R - \lambda_L q_L}{\lambda_R - \lambda_L} - \frac{1}{\lambda_R - \lambda_L}\left(\left(h_R u_R^2 + \frac{1}{2} g h_R^2\right) - \left(h_L u_L^2 + \frac{1}{2} g h_L^2\right)\right). \tag{36}$$

Then, both relations (33) and (34) reformulate as follows:

$$\lambda_R h_R^* - \lambda_L h_L^* = (\lambda_R - \lambda_L) h^{HLL}, \tag{37}$$

$$\lambda_R q_R^* - \lambda_L q_L^* = (\lambda_R - \lambda_L) q^{HLL} + \Delta x \bar{S}_{LR}^q. \tag{38}$$

Let us emphasize that the full determination of $\widetilde{w}_{\mathcal{R}}$ is achieved as soon as the two intermediate states, (h_L^*, q_L^*) and (h_R^*, q_R^*), are fixed. As a consequence, we have to define four values while, at this level, we have two equations (37) and (38). Clearly, two relations are missing. We must also preserve the steady states. Hence, we formally adopt the local steady state definition (19) to propose suitable closure relations. First, we note that the discharge must be constant to define a steady state. Then, concerning the intermediate discharge we adopt the following equalities:

$$q_L^* = q_R^* = q^*. \tag{39}$$

Because of (38), the intermediate discharge is then given by

$$q^* = q^{HLL} + \frac{\Delta x \bar{S}_{LR}^q}{(\lambda_R - \lambda_L)}. \tag{40}$$

Now, concerning the evaluation of the intermediate water heights, h_L^* and h_L^*, we have the equation (37) to be supplemented with an additional relation such that the pair (h_L^*, h_R^*) is solution of (2×2) system. Our objective is to propose a relevant additional equation such that $h_L^* = h_L$ and $h_R^* = h_R$ is the unique solution as soon as (w_L, w_R, z_L, z_R) verifies (19). For instance, in [3], the expected second equation is given by $\mathcal{B}(w_L^*, z_L) = \mathcal{B}(w_R^*, z_R)$. But such a choice involves strong nonlinearities. After [22, 23], this nonlinear system can be substituted by a linear system which preserve all the required properties. In [22, 23], the authors adopt the following additional relation:

$$h_R^* - h_L^* = \frac{\Delta x \bar{S}_{LR}^q}{\alpha_{LR}}, \tag{41}$$

where

$$\alpha_{LR} = g\bar{h} - \frac{\overline{q^2}}{h_L h_R}, \tag{42}$$

where $\overline{q^2}$ is defined by (31). The 2×2 linear system made of (37) and (41) does not admit a unique solution as long as $\overline{q^2} = g\bar{h} h_L h_R$. As a consequence, we suggest the following improvement:

$$h_R^* - h_L^* = \frac{\alpha_{LR} \Delta x \bar{S}_{LR}^q}{\alpha_{LR}^2 + \varepsilon_{LR} \Delta x^k}. \tag{43}$$

At the main discrepancy with (41), we remark that the right hand side in (43) is well-defined. Indeed, if $\alpha_{LR}^2 + \varepsilon_{LR}\Delta x^k = 0$, necessarily we have $\alpha_{LR} = 0$ and $\varepsilon_{LR} = 0$. But $\varepsilon_{LR} = 0$ holds if and only if (19) is satisfied. Then, according to (24), we have $\Delta x \bar{S}_{LR}^q = \alpha_{LR}(h_R - h_L)$, and as a consequence, we get

$$\lim_{\alpha_{LR},\varepsilon_{LR}\to 0} \frac{\alpha_{LR}\Delta x \bar{S}_{LR}^q}{\alpha_{LR}^2 + \varepsilon_{LR}\Delta x^k} = h_R - h_L. \tag{44}$$

To conclude, h_L^* and h_R^* are given as solution of the 2×2 linear system made of (37) and (43). The solution is directly given by

$$h_L^* = h^{HLL} + \frac{\lambda_R \Delta x \bar{S}_{LR}^q \alpha_{LR}}{(\lambda_R - \lambda_L)(\alpha_{LR}^2 + \varepsilon_{LR}\Delta x^k)}, \tag{45}$$

$$h_R^* = h^{HLL} + \frac{\lambda_L \Delta x \bar{S}_{LR}^q \alpha_{LR}}{(\lambda_R - \lambda_L)(\alpha_{LR}^2 + \varepsilon_{LR}\Delta x^k)}. \tag{46}$$

However, such an evaluation of the intermediate water heights does not ensure the required positiveness of h_L^* and h_R^*. Here, we adopt a positive cutoff introduce in [3] (see also [4, 22, 23]). As a consequence, h_L^* and h_R^* are corrected as follows:

$$h_L^* = \min\left(\max\left(h^{HLL} + \frac{\lambda_R \Delta x \bar{S}_{LR}^q \alpha_{LR}}{(\lambda_R - \lambda_L)(\alpha_{LR}^2 + \varepsilon_{LR}\Delta x^k)}, \sigma\right), \left(1 - \frac{\lambda_R}{\lambda_L}\right) h^{HLL} + \frac{\lambda_R}{\lambda_L}\sigma\right) \tag{47}$$

$$h_R^* = \min\left(\max\left(h^{HLL} + \frac{\lambda_L \Delta x \bar{S}_{LR}^q \alpha_{LR}}{(\lambda_R - \lambda_L)(\alpha_{LR}^2 + \varepsilon_{LR}\Delta x^k)}, \sigma\right), \left(1 - \frac{\lambda_L}{\lambda_R}\right) h^{HLL} + \frac{\lambda_L}{\lambda_R}\sigma\right) \tag{48}$$

where $\sigma = \min(h_L, h_R, h^{HLL})$.

Now, let us remark that $h^{HLL} > 0$ as long as the exact water height Riemann solution $h_{\mathcal{R}}$ remains positive. Moreover, by definition of σ, we have $\sigma - h^{HLL} \leq 0$. Since $\lambda_L < 0 < \lambda_R$ then we get

$$\left(1 - \frac{\lambda_R}{\lambda_L}\right) h^{HLL} + \frac{\lambda_R}{\lambda_L}\sigma = h^{HLL} + \frac{\lambda_R}{\lambda_L}\left(\sigma - h^{HLL}\right) > 0,$$
$$\left(1 - \frac{\lambda_L}{\lambda_R}\right) h^{HLL} + \frac{\lambda_L}{\lambda_R}\sigma = h^{HLL} + \frac{\lambda_L}{\lambda_R}\left(\sigma - h^{HLL}\right) > 0.$$

As a consequence, we immediately get $h_L^* > 0$ and $h_R^* > 0$.

In addition to this positiveness statement, it is worth noticing that the proposed water height cut-off correction preserves the conservation since the relation (37), or equivalently (33), always is satisfied. To establish (37), for the sake of simplicity in the notations, let us set

$$\Sigma_{LR} = \frac{\lambda_L \lambda_R \Delta x \bar{S}_{LR}^q \alpha_{LR}}{(\lambda_R - \lambda_L)(\alpha_{LR}^2 + \varepsilon_{LR}\Delta x^k)},$$

so that we have

$$\begin{aligned}\lambda_R h_R^\star - \lambda_L h_L^\star =& \min\left(\max\left(\lambda_R h^{HLL} + \Sigma_{LR}, \lambda_R\sigma\right), (\lambda_R-\lambda_L)h^{HLL} + \lambda_L\sigma\right)\\ &+ \min\left(\max\left(-\lambda_L h^{HLL} - \Sigma_{LR}, -\lambda_L\sigma\right), (\lambda_R-\lambda_L)h^{HLL} - \lambda_R\sigma\right).\end{aligned}$$

The above quantity is easily evaluated by comparing Σ_{LR}, $\lambda_R(\sigma - h^{HLL})$ and $\lambda_L(\sigma - h^{HLL})$. Indeed, let us first assume

$$\lambda_R(\sigma - h^{HLL}) < \Sigma_{LR} < \lambda_L(\sigma - h^{HLL}). \tag{49}$$

Then we get

$$\begin{aligned}&\max\left(\lambda_R h^{HLL} + \Sigma_{LR}, \lambda_R\sigma\right) = \lambda_R h^{HLL} + \Sigma_{LR},\\ &\max\left(-\lambda_L h^{HLL} - \Sigma_{LR}, -\lambda_L\sigma\right) = -\lambda_L h^{HLL} - \Sigma_{LR}.\end{aligned}$$

Moreover, we easily notice that the assumption (49) imposes

$$\begin{aligned}&\lambda_R h^{HLL} + \Sigma_{LR} \le (\lambda_R-\lambda_L)h^{HLL} + \lambda_L\sigma,\\ &-\lambda_L h^{HLL} - \Sigma_{LR} \le (\lambda_R-\lambda_L)h^{HLL} - \lambda_R\sigma,\end{aligned}$$

to recover the conservation relation (37).

Now, let us assume

$$\Sigma_{LR} < \lambda_R(\sigma - h^{HLL}) < \lambda_L(\sigma - h^{HLL}), \tag{50}$$

to get

$$\begin{aligned}&\max\left(\lambda_R h^{HLL} + \Sigma_{LR}, \lambda_R\sigma\right) = \lambda_R\sigma,\\ &\max\left(-\lambda_L h^{HLL} - \Sigma_{LR}, -\lambda_L\sigma\right) = -\lambda_L h^{HLL} - \Sigma_{LR}.\end{aligned}$$

In addition, according to (50), from a direct evaluation, we obtain

$$\begin{aligned}&\lambda_R\sigma \le (\lambda_R-\lambda_L)h^{HLL} + \lambda_L\sigma,\\ &-\lambda_L h^{HLL} - \Sigma_{LR} \ge (\lambda_R-\lambda_L)h^{HLL} - \lambda_R\sigma,\end{aligned}$$

and once again we recover the expected relation (37). We here skip the last assumption $\lambda_R(\sigma - h^{HLL}) < \lambda_L(\sigma - h^{HLL}) < \Sigma_{LR}$ since the establishment of (37) is similar to the above case with (50).

The definition of the approximate Riemann solver (32) is now achieved. To conclude this section, we establish that the approximate Riemann solver preserves the steady solutions.

Lemma 4.1 Let w_L and w_R be given in Ω. Consider the approximate Riemann solver in the form (32) where the intermediate states are given by (40), (47) and (48). If (w_L, w_R, z_L, z_R) satisfy the local steady state condition (19) with $\bar{F}_r \neq 1$, then the approximate Riemann solver stays at rest, namely we have

$$\widetilde{w}_{\mathcal{R}}(x/\Delta t; w_L, w_R, z_L, z_R) = \begin{cases} w_L \text{ if } x < 0\\ w_R \text{ if } x > 0.\end{cases} \tag{51}$$

Proof Since the local steady condition (19) is satisfied, the topography source term, given by (30), reads

$$\Delta x \bar{S}^q_{LR} = -g\bar{h}(z_R - z_L) - \frac{q^2}{4h_L^2 h_R^2} \times \frac{(h_L - h_R)(z_R - z_L)^2}{(1 - \bar{F}_r^2)^2},$$

where $q = q_L = q_R$. As long as $\bar{F}_r \neq 1$, arguing Lemma 3.1, $\bar{S}^q_{LR}$ is now given by (21). Then, from (40), straightforward computations gives $q^* = q$, and then the discharge is stationary. Concerning the intermediate water height, since the local steady condition (5) is verified, we have the following equality:

$$h^{HLL} - \frac{\lambda_{L,R}}{\lambda_R - \lambda_L}\Delta x \bar{S}^q_{LR}\frac{\alpha_{LR}}{\alpha_{LR}^2 + \varepsilon_{LR}\Delta x^k} = \frac{1}{2}(h_L + h_R) - \frac{\lambda_{L,R}}{\lambda_R - \lambda_L}\frac{\Delta x \bar{S}^q_{LR}}{\alpha_{LR}},$$

where α_{LR} is given by (42). For the sake of simplicity in the notations, we have set $\lambda_{L,R} = \lambda_L$ or λ_R. With $\alpha_{LR} \neq 0$, since the relation (24) holds, we directly obtain

$$h^{HLL} - \frac{\lambda_{L,R}}{\lambda_R - \lambda_L}\Delta x \bar{S}^q_{LR}\frac{\alpha_{LR}}{\alpha_{LR}^2 + \varepsilon_{LR}\Delta x^k} = h_{L,R}.$$

Then according to (47) and (48), we easily obtain $h_L^* = h_L$ and $h_R^* = h_R$, and the proof is achieved. □

5 Main properties of the scheme

Equipped with the approximate Riemann solver (32), where the intermediate states are given by (40), (47) and (48), supplemented with the source term discretization (30), then the scheme (18) is fully determined. Now, we state the main properties satisfied by the derived numerical approximation.

THEOREM 5.1 Assume the following CFL-like restriction:

$$\frac{\Delta t}{\Delta x}\max_{i\in\mathbb{Z}}\left(|\lambda^L_{i+1/2}|, |\lambda^R_{i+1/2}|\right) \leq \frac{1}{2}. \tag{52}$$

The scheme (18) is consistent with (1). Let w_i^n be in Ω for all $i \in \mathbb{Z}$. The updated states w_i^{n+1} given by the scheme (18), satisfy the following properties:

1. Positiveness preservation: $h_i^{n+1} > 0$ for all $i \in \mathbb{Z}$,
2. Preservation of all smooth steady states: $w_i^{n+1} = w_i^n$ for all $i \in \mathbb{Z}$ as soon as $(w_i^n)_{i\in\mathbb{Z}}$ verifies

$$q_i^n = Q \qquad \text{and} \qquad \frac{(q_i^n)^2}{2(h_i^n)^2} + g(h_i^n + z_i) = B \qquad \text{for all } i \in \mathbb{Z}, \tag{53}$$

   for given constants Q and B.
3. An incomplete entropy inequality in the form:

$$\frac{\eta_i^{n+1} - \eta_i^n}{\Delta t} + \frac{G_{i+1/2} - G_{i-1/2}}{\Delta x} \leq -\bar{S}_i^\eta + \mathcal{O}(\Delta x), \tag{54}$$

is satisfied as long as

$$h_{i+1/2}^{HLL}+\frac{\lambda_{i+1/2}^{L}\Delta x\bar{S}_{i+1/2}^{q}\alpha_{i+1/2}}{\alpha_{i+1/2}^{2}+\varepsilon_{i+1/2}\Delta x^{k}}>0\quad\text{and}\quad h_{i+1/2}^{HLL}+\frac{\lambda_{i+1/2}^{R}\Delta x\bar{S}_{i+1/2}^{q}\alpha_{i+1/2}}{\alpha_{i+1/2}^{2}+\varepsilon_{i+1/2}\Delta x^{k}}>0, \tag{55}$$

where we have set

$$G_{i+1/2}=\frac{1}{2}(G(w_{i+1}^{n})+G(w_{i}^{n}))+\frac{\Delta x}{4\Delta t}(\eta(w_{i+1}^{n})-\eta(w_{i}^{n}))+\frac{\Delta x}{2\Delta t}(I_{i+1/2}^{\eta^{+}}-I_{i-1/2}^{\eta^{-}}), \tag{56}$$

with

$$I_{i+1/2}^{\eta^{+}}=\frac{1}{\Delta x}\int_{0}^{\Delta x/2}\eta(\widetilde{w}_{\mathcal{R}}(\frac{x}{\Delta t};w_{i}^{n},w_{i+1}^{n},z_{i},z_{i+1}))\,dx, \tag{57}$$

$$I_{i+1/2}^{\eta^{-}}=\frac{1}{\Delta x}\int_{-\Delta x/2}^{0}\eta(\widetilde{w}_{\mathcal{R}}(\frac{x}{\Delta t};w_{i}^{n},w_{i+1}^{n},z_{i},z_{i+1}))\,dx, \tag{58}$$

and

$$\bar{S}_{i}^{\eta}=\frac{1}{2}\left(\frac{h_{i-1}^{n}+h_{i}^{n}}{2}\frac{q_{i-1/2}^{HLL}}{h_{i-1/2}^{HLL}}(\frac{z_{i}-z_{i-1}}{\Delta x})+\frac{h_{i}^{n}+h_{i+1}^{n}}{2}\frac{q_{i+1/2}^{HLL}}{h_{i+1/2}^{HLL}}(\frac{z_{i+1}-z_{i}}{\Delta x})\right). \tag{59}$$

Before we establish the above result, let us comment the discrete entropy inequality (54). Indeed, it is worth noticing that the residue, given by $\mathcal{O}(\Delta x)$, is governed by the smoothness of the topography function z and never depends on the unknowns (eventually discontinuous). As a consequence, the well-known Lax-Wendroff Theorem can be applied so that the converged solution turns out to be an entropy preserving weak solution of (1).

In addition, let us highlight the assumption (55) to get the discrete entropy inequality (54). In fact, (55) enforces the intermediate water heights to be given by (45) and (46) so that the cut-off corrections (47) and (48) stay inactive. Put in other words, we here present discrete entropy inequalities far away from the dry areas and wet/dry transitions.

Now, in order to establish the above result, we need the following technical lemma where we state the behavior of the entropy at each interface.

Lemma 5.1 Let w_L and w_R be in Ω such that h_L^* and h_R^*, defined by (47) and (48), coincide with (45) and (46). Let η and G be given by (3). Assume a CFL-like restriction in the form

$$\frac{\Delta t}{\Delta x}\max\left(|\lambda_L|,|\lambda_R|\right)\leq\frac{1}{2}. \tag{60}$$

The approximate Riemann solver (32) with the intermediate states given by (40), (47) and (48) verifies the following inequality:

$$\begin{aligned}\frac{1}{\Delta x}\int_{-\Delta x/2}^{\Delta x/2}\eta(\widetilde{w}_{\mathcal{R}}(x/\Delta t;w_L,w_R,z_L,z_R))\,dx\leq\frac{1}{2}(\eta(w_L)+\eta(w_R))\\-\frac{\Delta t}{\Delta x}(G(w_R)-G(w_L))-\Delta t\bar{S}_{LR}^{\eta}+\frac{\Delta t}{\Delta x}\mathcal{O}(\Delta x^{2}),\end{aligned} \tag{61}$$

where

$$\bar{S}_{LR}^{\eta}(\Delta x,w_L,w_R,z_L,z_R)=\frac{g\bar{h}q^{HLL}}{h^{HLL}}\times\frac{z_R-z_L}{\Delta x}. \tag{62}$$

Proof With an approximate Riemann solver given by (32), under the CFL-like condition (60) we immediately have

$$\begin{aligned}\frac{1}{\Delta x}\int_{-\Delta x/2}^{\Delta x/2}\eta(\widetilde{w}_{\mathcal{R}}(x/\Delta t;w_L,w_R,z_L,z_R))\,dx &= \left(\frac{1}{2}-\lambda_L\frac{\Delta t}{\Delta x}\right)\eta(w_L)\\ &+\frac{\Delta t}{\Delta x}\left(\lambda_R\eta(w_R^*)-\lambda_L\eta(w_L^*)\right)+\left(\frac{1}{2}-\lambda_R\frac{\Delta t}{\Delta x}\right)\eta(w_R).\end{aligned} \tag{63}$$

Now, we have

$$\eta(w_L^*)=\frac{(q^*)^2}{2h_L^*}+g\frac{(h_L^*)^2}{2}\qquad\text{and}\qquad\eta(w_R^*)=\frac{(q^*)^2}{2h_R^*}+g\frac{(h_R^*)^2}{2},$$

where q^* and $h_{L,R}^*$ are given by (40), (45) and (46). Since the topography function is smooth, then $z_R-z_L=\mathcal{O}(\Delta x)$. As a consequence, as long as $\alpha_{LR}\neq 0$, we have

$$\begin{aligned}q^* &= q^{HLL}-\frac{g\bar{h}}{\lambda_R-\lambda_L}(z_R-z_L)+\mathcal{O}(\Delta x^2),\\ h_R^* &= q^{HLL}+\frac{\lambda_L}{\lambda_R-\lambda_L}\frac{g\bar{h}}{\alpha_{LR}}(z_R-z_L)+\mathcal{O}(\Delta x^2),\\ h_L^* &= q^{HLL}+\frac{\lambda_R}{\lambda_R-\lambda_L}\frac{g\bar{h}}{\alpha_{LR}}(z_R-z_L)+\mathcal{O}(\Delta x^2).\end{aligned}$$

Then, straightforward computations give

$$\lambda_R\eta(w_R^*)-\lambda_L\eta(w_L^*)=(\lambda_R-\lambda_L)\eta(w^{HLL})-g\frac{\bar{h}q^{HLL}}{h^{HLL}}(z_R-z_L)+\mathcal{O}(\Delta x^2). \tag{64}$$

Moreover, after [20], we have

$$\eta(w^{HLL})\leq\frac{\lambda_R}{\lambda_R-\lambda_L}\eta(w_R)-\frac{\lambda_L}{\lambda_R-\lambda_L}\eta(w_L)-\frac{1}{\lambda_R-\lambda_L}(G(w_R)-G(w_L)),$$

so that

$$\begin{aligned}\lambda_R\eta(w_R^*)-\lambda_L\eta(w_L^*) \leq\ & \lambda_R\eta(w_R)-\lambda_L\eta(w_L)-(G(w_R)-G(w_L))\\ & -g\frac{\bar{h}q^{HLL}}{h^{HLL}}(z_R-z_L)+\mathcal{O}(\Delta x^2).\end{aligned} \tag{65}$$

The expected inequality (61) comes combining (63) with the above estimation. To complete the proof, let us underline that $h_L^*=h_R^*=h^{HLL}$ if $\alpha_{LR}=0$ so that the estimation (64) immediately holds. The proof is then achieved. □

Equipped with the above result, we are able to establish Theorem 5.1.

Proof First, we establish the consistency of the derived scheme (18). To address such an issue, first we notice that the CFL-like condition (52) ensures that the sequence of approximate Riemann solver are non-interacting. Next, we show the consistency of both numerical flux and source term. Concerning the numerical flux, we have

$$f_\Delta(w,w,z_L,z_R)=f(w)+\frac{\Delta x}{2\Delta t}(I_{LR}^+-I_{LR}^+),$$

where I^+_{LR} and I^-_{LR} are defined by (17) and (16). Since the approximate Riemann solver is in the form (32), then we get

$$f_\Delta(w, w, z_L, z_R) = f(w) + \frac{\lambda_R}{2}(w^*_R - w) + \frac{\lambda_L}{2}(w^*_L - w).$$

Arguing the definition of the intermediate states, with $w_L = w_R = w \in \Omega$, enforcing Δx to be small enough, we get

$$\begin{aligned}
q^* &= q - \frac{1}{\lambda_R - \lambda_L} gh(z_R - z_L), \\
h^*_L &= h + \frac{\lambda_R}{\lambda_R - \lambda_L} gh(z_R - z_L) \frac{gh - q^2/h^2}{(gh - q^2/h^2)^2 + \Delta x^k \sqrt{|z_R - z_L|}}, \\
h^*_L &= h + \frac{\lambda_R}{\lambda_R - \lambda_R} gh(z_R - z_L) \frac{gh - q^2/h^2}{(gh - q^2/h^2)^2 + \Delta x^k \sqrt{|z_R - z_L|}},
\end{aligned}$$

to immediately obtain the expected consistency of the numerical flux as follows:

$$\lim_{z_L, z_R \to z} f_\Delta(w, w, z_L, z_R) = f(w).$$

Next, concerning the consistency of the discrete source term, given by (30), as soon as $w_L = w_R = w$ we have

$$\bar{S}^q_{LR}(w, w, z_L, z_R) = -gh \frac{(z_R - z_L)}{\Delta x}.$$

With a smooth topography function, let us fix $z_L = z(x - \frac{\Delta x}{2})$ and $z_R = z(x + \frac{\Delta x}{2})$ so that we obtain

$$\lim_{\Delta x \to 0} \bar{S}^q_{LR}(w, w, z_L, z_R) = -gh\partial_x z,$$

and the scheme (18) is established to be consistent.

Now, we show the positiveness of h^{n+1}_i. After (11), since the intermediate water height, defined by (47)-(48), involved within the approximate Riemann solver, are positive, then h^{n+1}_i is nothing but the integral of the positive quantities. As a consequence, we get $h^{n+1}_i > 0$.

Next, concerning the well-balanced property, since $(w^n_i)_{i \in \mathbb{Z}}$ verify (53), at each interface the local steady condition (19) is satisfied. As a consequence of Lemma 4.1, all the non interacting approximate Riemann solution are steady so that we get

$$\widetilde{w}_{\mathcal{R}}\left(\frac{x - x_{i+1/2}}{\Delta t}; w^n_i, w^n_{i+1}, z_i, z_{i+1}\right) = \begin{cases} w^n_i & \text{if} \quad x_{i+1/2} < 0, \\ w^n_{i+1} & \text{if} \quad x_{i+1/2} > 0. \end{cases} \tag{66}$$

Then we have the following sequence of equalities

$$\begin{aligned}
w^{n+1}_i &= \frac{1}{\Delta x} \int_{x_{i-1/2}}^{x_i} \widetilde{w}_{\mathcal{R}}(\frac{x - x_{i-1/2}}{\Delta t}; w^n_{i-1}, w^n_i, z_{i-1}, z_i)\, dx \\
&\quad + \frac{1}{\Delta x} \int_{x_i}^{x_{i+1/2}} \widetilde{w}_{\mathcal{R}}(\frac{x - x_{i+1/2}}{\Delta t}; w^n_i, w^n_{i+1}, z_i, z_{i+1})\, dx, \\
&= w^n_i.
\end{aligned}$$

To conclude the proof, we establish the entropy inequality (54). Since the entropy function η is convex, the well-known Jensen inequality gives

$$\begin{aligned}\eta(w_i^{n+1}) &\leq \frac{1}{\Delta x}\int_{x_{i-1/2}}^{x_{i+1/2}} \eta(w_{\mathcal{R}}^{\Delta}(x,t^n+\Delta t))\,dx,\\ &\leq \frac{1}{\Delta x}\int_0^{\Delta x/2} \eta(\tilde{w}_{\mathcal{R}}(\frac{x}{\Delta t};w_{i-1}^n,w_i^n,z_{i-1},z_i))\,dx\\ &\quad+\frac{1}{\Delta x}\int_{-\Delta x/2}^{0} \eta(\tilde{w}_{\mathcal{R}}(\frac{x}{\Delta t};w_i^n,w_{i+1}^n,z_i,z_{i+1}))\,dx,\end{aligned}$$

so that, arguing (57) and (58), we obtain

$$\begin{aligned}\eta(w_i^{n+1}) \leq \frac{1}{2}(I_{i-1/2}^{\eta^-}+I_{i-1/2}^{\eta^+})+\frac{1}{2}(I_{i-1/2}^{\eta^+}-I_{i-1/2}^{\eta^-})\\ +\frac{1}{2}(I_{i+1/2}^{\eta^-}+I_{i+1/2}^{\eta^+})-\frac{1}{2}(I_{i+1/2}^{\eta^+}-I_{i+1/2}^{\eta^-}).\end{aligned} \tag{67}$$

Next, because of (55), necessarily the intermediate water heights, given by (45) and (46), are positive. Since the positive water height cut-off corrections (47) and (48) is not active then Lemma 5.1 can be applied. As a consequence, from (61), we deduce

$$\begin{aligned}I_{i+1/2}^{\eta^-}+I_{i+1/2}^{\eta^+} &\leq \frac{1}{2}(\eta(w_i^n))+\eta(w_{i+1}^n))-\frac{\Delta t}{\Delta x}(G(w_{i+1}^n))-G(w_i^n)\\ &\quad-\Delta t\bar{S}_{LR}^{\eta}+\frac{\Delta t}{\Delta x}\mathcal{O}(\Delta x^2),\end{aligned}$$

where, according to (59), we have set $\bar{S}_{i+1/2}^{\eta}=\bar{S}_{LR}^{\eta}(\Delta x,w_i^n,w_{i+1}^n,z_i,z_{i+1})$. Now, by introducing the above estimation in (67), after straightforward computation, we obtain the expected discrete entropy inequality (54). The proof is then achieved. □

6 Numerical experiments

In this section, we perform several numerical experiments to illustrate the behavior of the designed fully well-balanced corrected scheme (FWBC). A comparison with the well-known hydrostatic reconstruction (HR) method [1], applied to the HLL scheme [20], and the well-balanced scheme (FWB) proposed in [22, 23], is displayed for all the simulations. Concerning the FWB-scheme, according to the source term discretization given by (7) and (8), a parameter denoted C must be fix. In the present work, all the displayed numerical simulations are performed considering $C \in [1, 2.5]$ according to the realized simulations. We emphasize that spurious oscillations appear with $C \geq 5$ while the approximate solutions blow-up with $C \geq 10$. Once again, we underline that the proposed correction of the FWB-scheme is now free from this parameter C.

As long as the exact solution is known, the behavior of the obtained approximate solutions is exhibited by evaluating the L^1, L^2 and L^∞ errors. Such errors are given

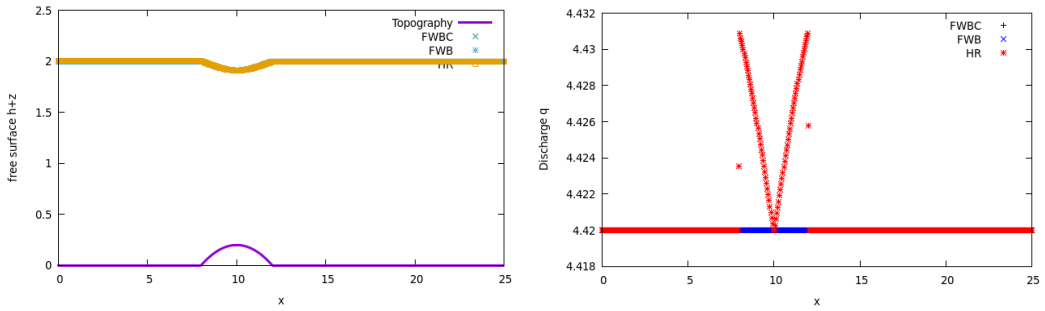

(a) (b)

Figure 3: Free surface (3a) and discharge (3b) for the simulation of a subcritical flow.

by

$$||w^n - w^{ex}(.,t^n)||_{L^1} = \sum_{i\in\mathbb{Z}} |w_i^n - w^{ex}(x_i,t^n)|\Delta x, \tag{68}$$

$$||w^n - w^{ex}(.,t^n)||_{L^2} = \sqrt{\sum_{i\in\mathbb{Z}} (w_i^n - w^{ex}(x_i,t^n))^2 \Delta x}, \tag{69}$$

$$||w^n - w^{ex}(.,t^n)||_{L^\infty} = \max_{i\in\mathbb{Z}} |w_i^n - w^{ex}(x_i,t^n)|, \tag{70}$$

where $(w_i^n)_{i\in\mathbb{Z}}$ is defined by the adopted numerical scheme while $w^{ex}(x,t)$ denotes the expected exact solution.

6.1 The subcritical flow

This test is used to see the ability of the scheme to capture steady states. The domain is $[0,25]$ and the topography is defined by $z(x) = (0, 0.2 - 0.05(x-10)^2)_+$ where $x_+ = \max(0,x)$. The initial conditions are $h(x,0) = 2$ and $q(x,0) = 4.42$. On the left boundary condition, the water height satisfies a homogeneous Neumann condition and the discharge is equal to $q_0 = 4.42$. On the right boundary, the water height is equal to $h_0 = 2$ and the discharge follows a homogeneous Neumann boundary condition.

	$h+z$			q		
	L^1_{error}	L^2_{error}	L^∞_{error}	L^1_{error}	L^2_{error}	L^∞_{error}
HR-scheme	1.32e-02	1.36e-02	1.59e-02	2.89e-03	2.89e-03	2.89e-02
FWB-scheme	1.15e-13	1.20e-13	1.51e-13	6.63e-14	6.99e-14	8.26e-14
FWBC-scheme	1.10e-13	1.17e-13	1.44e-13	6.57e-14	6.84e-14	8.21e-14

Table 1: Free surface and discharge errors for the subcritical flow.

The domain is here discretized with 1000 cells. At times $t = 100$, so that the steady regime is researched, the approximate solutions are displayed in Figure 3. In Table 1, we present the numerical errors. We note that the approximate solution given

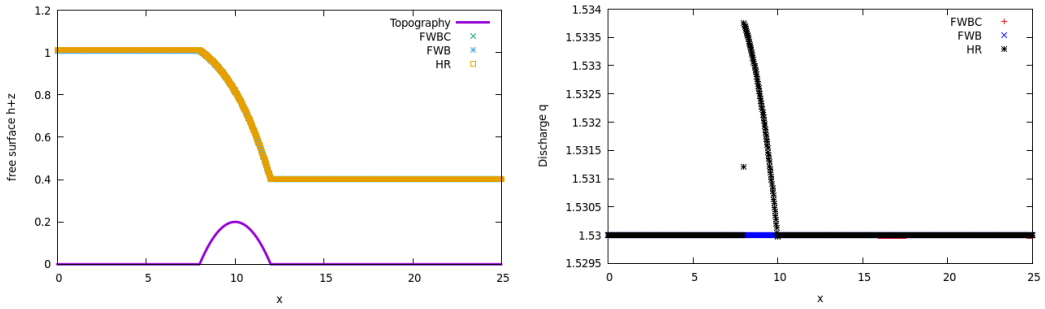

(a) (b)

Figure 4: Free surface (4a) and discharge (4b) for the simulation of a transcritical flow without shock.

by the fully well-balanced scheme (18) is in very good agreements with the exact solution since such a scheme exactly preserves this solution.

6.2 The transcritical flow without shock

We consider a computational domain given by $[0, 25]$ and the topography is defined by $z(x) = (0, 0.2 - 0.05(x - 10)^2)_+$. We consider the initial data given by $h(x, 0) = 0.66$ and $q(x, 0) = 1.53$. On the left boundary condition, the water height satisfies a homogeneous Neumann condition and the discharge is equal to $q_0 = 1.53$. On the right boundary, the water height is equal to $h_0 = 0.66$ and the discharge follows a homogeneous Neumann boundary condition. The obtained numerical simulation are displayed Figure 4 at time $t = 500$ with 1000 cells.

	$h + z$			q		
	L^1_{error}	L^2_{error}	L^∞_{error}	L^1_{error}	L^2_{error}	L^∞_{error}
HR-scheme	4.79e-02	6.07e-02	8.12e-02	8.28e-04	3.30e-03	1.82e-02
FWB-scheme	1.67e-14	2.13e-14	4.26e-14	1.47e-14	1.58e-14	2.04e-14
FWBC-scheme	1.27e-14	1.67e-14	3.14e-14	1.27e-14	1.48e-14	1.98e-14

Table 2: Free surface and discharge errors for the transcritical flow without shock.

Once again, the fully well-balanced corrected scheme gives very good agreement with the exact solution in the steady regime which is exactly captured by the here derived scheme. The very good behavior of the numerical solution is highlight by Table 2 where the numerical errors are given.

6.3 The perturbed transcritical flow without shock

In this numerical simulation, we test the behavior of the derived scheme to deal with a perturbed stationary solution. Here, the initial data is given by $h(x, 0) = h_0(x) + h_\delta(x)$ and $q(x, 0) = q_0(x) + q_\delta(x)$ where (h_0, q_0) stands for the stationary solution of a transcritical flow without shock according to the numerical experiment

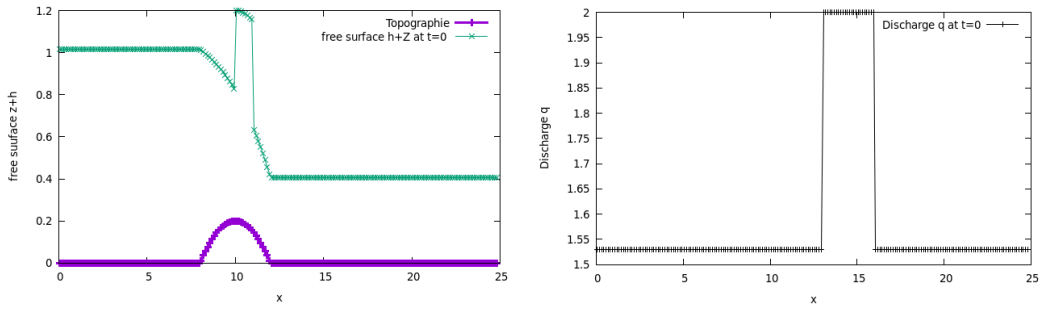

(a) (b)

Figure 5: Initial free surface (5a) and discharge (5b) for the the perturbed transcritical flow without shock.

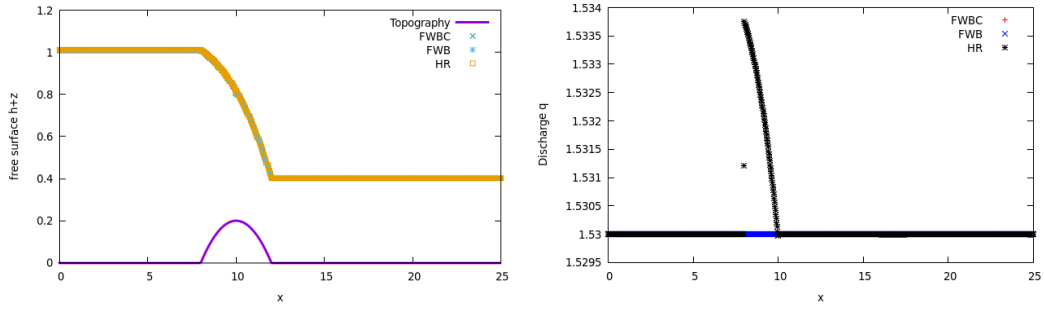

(a) (b)

Figure 6: Free surface (6a) and discharge (6b) for the the perturbed transcritical flow without shock.

presented Section 6.2 and (h_δ, q_δ) given by

$$h_\delta(x) = \begin{cases} 1 & \text{if} \quad 10 < x < 11, \\ 0 & \text{otherwise,} \end{cases} \qquad \text{and} \qquad q_\delta(x) = \begin{cases} 2 & \text{if} \quad 13 < x < 16, \\ 0 & \text{otherwise.} \end{cases}$$

This initial data is displayed Figure 5.

The resulting numerical approximations obtained with a mesh made of 200 cells for the HR-scheme, the FWB-scheme and FWBC-scheme at time $t = 500$ are displayed Figure 6. After a long time, the stationary solution is recovered according to the scheme accuracy (see also Table 3).

	$h+z$			q		
	L^1_{error}	L^2_{error}	L^∞_{error}	L^1_{error}	L^2_{error}	L^∞_{error}
HR-scheme	4.89e-02	6.17e-02	8.22e-02	8.38e-04	3.43e-03	1.98e-02
FWB-scheme	2.79e-14	2.85e-14	4.20e-14	1.62e-14	1.85e-14	2.18e-14
FWBC-scheme	2.77e-14	2.87e-14	4.14e-14	1.58e-14	1.75e-14	2.08e-14

Table 3: Free surface and discharge errors for the perturbed transcritical flow without shock.

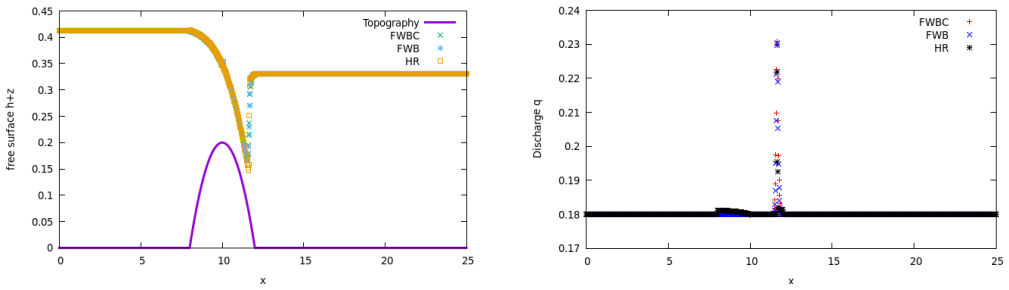

(a) (b)

Figure 7: Free surface (7a) and discharge (7b) for the simulation of a transcritical flow with shock.

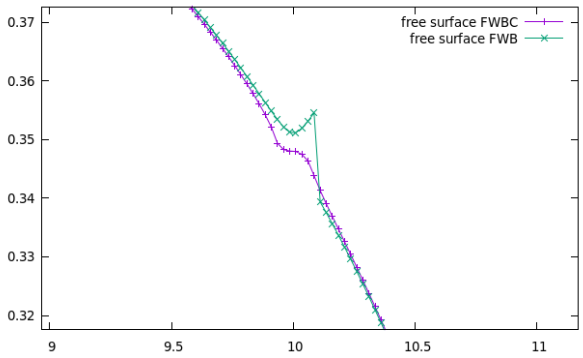

Figure 8: Zoom of the spurious perturbation of the water height produced by the ill-posed quantity $\mathcal{P} = g\frac{h_i^n+h_{i+1}^n}{2} - \frac{(q_i^n)^2+(q_{i+1}^n)^2}{2h_i^n h_{i+1}^n}$ with respect to the made correction.

6.4 Transcritical flow with shock

In this simulation, we show the behavior of an hydraulic jump approximation. The domain of the computation is $[0, 25]$ and the topography fixed by $z(x) = (0, 0.2 - 0.05(x - 10)^2)_+$. The initial data are given by $h(x, 0) = 0.33$ and $q(x, 0) = 0.18$. On the left boundary condition, the water height satisfies a homogeneous Neumann condition and the discharge is equal to $q_0 = 0.18$. On the right boundary, the water height is equal to $h_0 = 0.33$ and the discharge follows a homogeneous Neumann boundary condition.

	$h+z$			q		
	L^1_{error}	L^2_{error}	L^∞_{error}	L^1_{error}	L^2_{error}	L^∞_{error}
HR-scheme	1.16e-03	1.82e-03	5.12e-02	1.54e-04	1.53e-03	4.00e-02
FWB-scheme	2.81e-03	3.01e-03	9.85e-02	2.94e-04	3.35e-03	5.39e-02
FWBC-scheme	2.49e-03	2.40e-03	8.84e-02	2.851e-04	3.65e-03	5.08e-02

Table 4: Free surface and discharge errors for the transcritical flow with shock.

The numerical simulation obtained at time $t = 1000$ with the fully well-balanced scheme are displayed Figure 7. It is worth noting that the failure of scheme detected

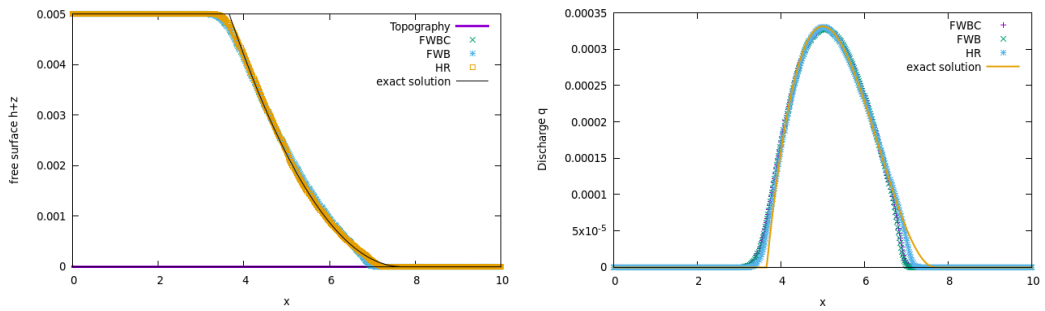

(a) (b)

Figure 9: Free surface (9a) and discharge (9b) for the dam-break on a dry domain.

in [22, 23] and illustrated Figure 2, is now corrected. Indeed, in Figure 8, we notice that the spurious perturbation no longer stays. The good behavior of the scheme is highlight by the errors evaluations given Table 4.

6.5 Wet/dry transition flow

According to [22, 23], we impose a vanishing velocity as soon as the water height vanishes. In addition, we have enforced $\frac{u}{h} = 0$ in the limit of h to zero. As a consequence, in a wet/dry transition interface, with $h_L = 0$ or $h_R = 0$, we get

$$\Delta x \bar{S}^q_{LR} = -g\bar{h}(z_R - z_L) \qquad \text{and} \qquad \alpha_{LR} = g\bar{h}, \tag{71}$$

so that all required properties, stated Theorem 5.1, are preserved.

6.5.1 Dam-break on a dry domain

This numerical experiment illustrates the ability of the scheme to correctly locate and treat the wet/dry transition. The domain is $[0, 10]$ with a flat topography. The initial data is made of a vanishing discharge in the whole domain while the water height is defined by

$$h(x, 0) = \begin{cases} 0.005 & \text{if } 0 < x < 5, \\ 0 & \text{if } 5 < x < 10. \end{cases}$$

We adopt homogeneous Neumann boundary conditions.

	$h+z$			q		
	L^1_{error}	L^2_{error}	L^∞_{error}	L^1_{error}	L^2_{error}	L^∞_{error}
HR-scheme	7.06e-5	5.20e-5	1.33e-4	1.33e-5	1.15e-5	2.92e-5
FWB-scheme	1.50e-4	9.54e-5	1.92e-4	2.62e-5	2.11e-5	4.17e-5
FWBC-scheme	1.51e-4	9.54e-5	1.92e-4	2.62e-5	2.11e-5	4.18e-5

Table 5: Free surface and discharge errors for the dam-break on a dry domain.

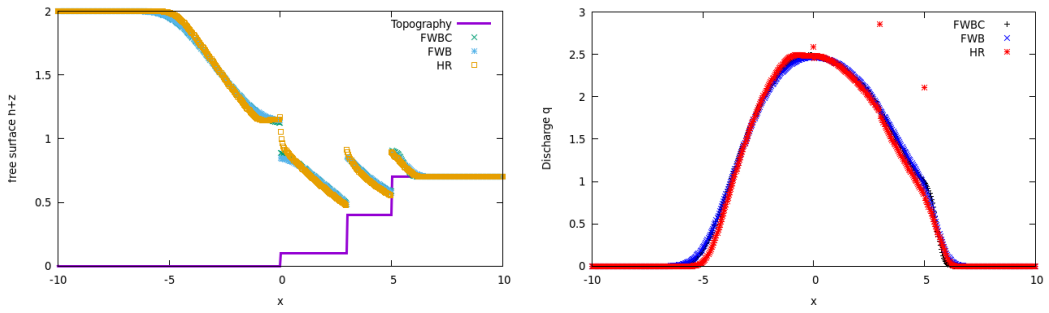

(a) (b)

Figure 10: Free surface (10a) and discharge (10b) for dam-break test case on steps topography.

The domain is here discritized with 500 cells and the obtained approximate solution at time $t = 6$ is displayed Figure 9. We notice the ability of the FWBC-scheme to deal with wet/dry transition and the here proposed correction preserves the relevance of the numerical method (see Table 5).

6.5.2 Dam-break on a step topography

This numerical simulation is devoted to illustrate the relevance of the scheme approximating the solution when the topography function is discontinuous. Here, in the domain $[-10, 10]$, the topography is made of three successive steps as follows:

$$z(x) = \begin{cases} 0 & \text{if } x < 0, \\ 0.1 & \text{if } 0 < x < 3, \\ 0.4 & \text{if } 3 < x < 5, \\ 0.7 & \text{if } x > 5. \end{cases}$$

The initial discharge is vanishing in the whole domain and the initial water height is defined by

$$h(x, 0) = \begin{cases} 1 & \text{if } x < 0, \\ 0 & \text{if } x > 0. \end{cases}$$

We consider homogeneous Neumann boundary conditions. The approximate solution for the free surface and the discharge are displayed Figure 10. We notice the good behaviors of both HR-scheme and FWBC-scheme while the discharge of the original FWB-scheme presents spurious values located at the discontinuities of the topography function. In Figure 11, we display the behavior of the time step Δt throughout the simulation. We remark that the derived correction does not drastically modify the behavior of Δt.

6.5.3 Lake at rest with an emerged bottom

In the computational domain $[0, 25]$, the bottom is defined by $z(x) = (0, 0.2 - 0.05(x - 10)^2)_+$. For the initial water height, we adopt $h(x, 0) = (0.15 - z(x))_+$ so

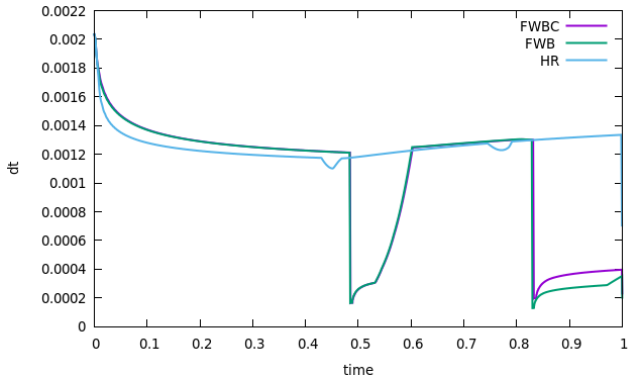

Figure 11: Evolution of the time step Δt versus time during the simulation of the dam-break test case on steps topography.

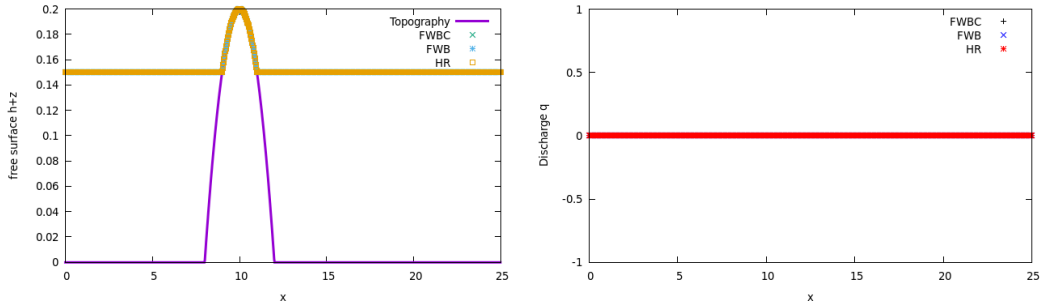

(a) (b)

Figure 12: Free surface (12a) and discharge (12b) for the lake at rest with emerged bottom.

that this simulation contains an emerged bottom. Concerning the initial discharge, we impose a vanishing velocity in the whole domain. We consider the homogeneous Neumann boundary conditions.

	$h+z$			q		
	L^1_{error}	L^2_{error}	L^∞_{error}	L^1_{error}	L^2_{error}	L^∞_{error}
HR-scheme	2.78e-19	2.78e-18	2.78e-17	2.60e-17	2.89e-17	4.58e-17
FWB-scheme	3.11e-17	5.01e-17	8.33e-17	2.72e-17	3.69e-17	1.02e-16
FWBC-scheme	2.11e-19	2.81e-18	3.33e-18	2.75e-19	3.01e-18	3.82e-18

Table 6: Free surface and discharge errors for the lake at rest with an emerged bottom.

In Figure 12 we display the approximate solution with 500 cells at time $t = 100$. According to the errors presented Table 6, the solution is exactly captured.

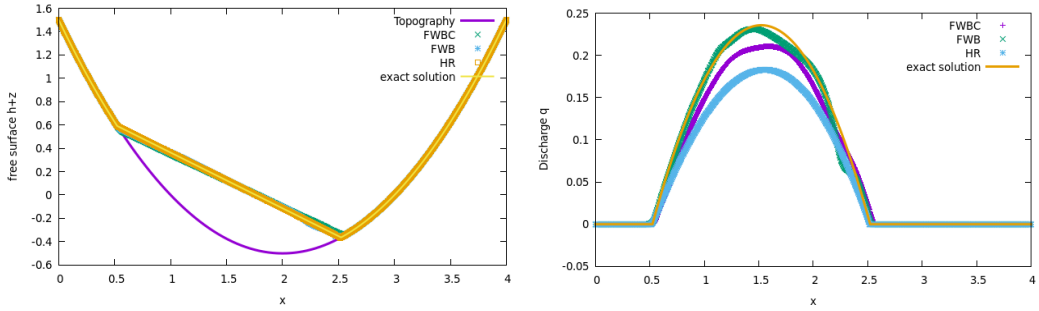

(a) (b)

Figure 13: Both exact and approximate free surface (13a) and both exact and approximate discharge (13b) for the Thacker test case.

6.5.4 Thacker test case

The computational domain is $[0, L]$ and the topography is defined by

$$z(x) = h_0 \left(\frac{1}{a^2} \left(x - \frac{L}{2} \right)^2 - 1 \right),$$

where h_0, a and L are parameters to be fixed. The exact solution is an oscillation of the free surface between the points

$$x_1(t) = -\frac{b}{w}\cos(wt) - a + \frac{L}{2} \qquad \text{and} \qquad x_2(t) = -\frac{b}{w}\cos(wt) + a + \frac{L}{2},$$

where $w = \sqrt{2gh_0}/a$, $b = w/2$ and the period $T = 2\pi/w$. The initial conditions are given by $q(x, 0) = 0$ and

$$h(x,0) = \begin{cases} -\dfrac{h_0}{a^2}\left(\left((x - \dfrac{L}{2}) + \dfrac{b}{\sqrt{2gh_0}} \right)^2 - a^2 \right) & \text{if } x_1(0) < x < x_2(0), \\ 0 & \text{otherwise.} \end{cases}$$

The exact water height is given by

$$h(x,t) = \begin{cases} -\dfrac{h_0}{a^2}\left(\left((x - \dfrac{L}{2}) + \dfrac{b}{\sqrt{2gh_0}} cos(wt) \right)^2 - a^2 \right) & \text{if } x_1(t) < x < x_2(t), \\ 0 & \text{otherwise,} \end{cases}$$

while the exact velocity reads

$$u(x,t) = \begin{cases} b\sin(wt) & \text{if } x_1(t) < x < x_2(t), \\ 0 & \text{otherwise.} \end{cases}$$

Concerning the parameters, we fix $a = 1$, $L = 4$ and $h_0 = 1/2$. In Figure 13, the approximate solution is displayed at time $t = 10.0303$ with 1000 cells.

	FWBC-scheme		
	q		
cells	L^1_{error}	L^2_{error}	L^∞_{error}
1600	3.74e-2	2.76e-2	2.64e-2
2000	2.66e-2	1.97e-2	1.94e-2
4000	1.15e-2	8.56e-3	9.51e-3

Table 7: Discharge errors for the Thacker test case for different cells using FWBC-scheme.

	FWB-scheme		
	q		
cells	L^1_{error}	L^2_{error}	L^∞_{error}
1600	1.24e-2	1.31e-2	3.30e-2
2000	1.10e-2	1.16e-2	2.99e-2
4000	7.98e-3	7.88e-3	2.19e-2

Table 8: Discharge errors for the Thacker test case for different cells using FWB-scheme.

	HR-scheme		
	q		
cells	L^1_{error}	L^2_{error}	L^∞_{error}
1600	7.29e-2	5.59e-2	5.36e-2
2000	5.83e-2	4.47e-2	4.48e-2
4000	2.91e-2	2.23e-2	2.13e-2

Table 9: Discharge errors for the Thacker test case for different cells using HR-scheme.

Concerning the water height, displayed in Figure 13a, we obtain a good approximation of the wet/dry transition. Now, the approximation of the discharge is not good as expected. However, we recall that usual method like the hydrostatic reconstruction cannot give good approximation of the discharge. In Tables 7, 8 and 9, we present the obtained errors for q. We notice that the here designed FWBC-scheme produces better approximation than the hydrostatic reconstruction scheme.

6.6 Drain on a non-flat bottom

This numerical experiment is proposed in [13], where the topography is defined by $z(x) = (0.2 - 0.05(x-10)^2)_+$ over a computational domain given by [0,25]. The initial data is fixed as follows:

$$h(x,0) + z(x) = 0.5 \qquad \text{and} \qquad q(x,0) = 0.$$

Concerning the boundary conditions, according in [13], the left boundary condition is given by

$$h_L = h_1^n \qquad \text{and} \qquad q_L = 0,$$

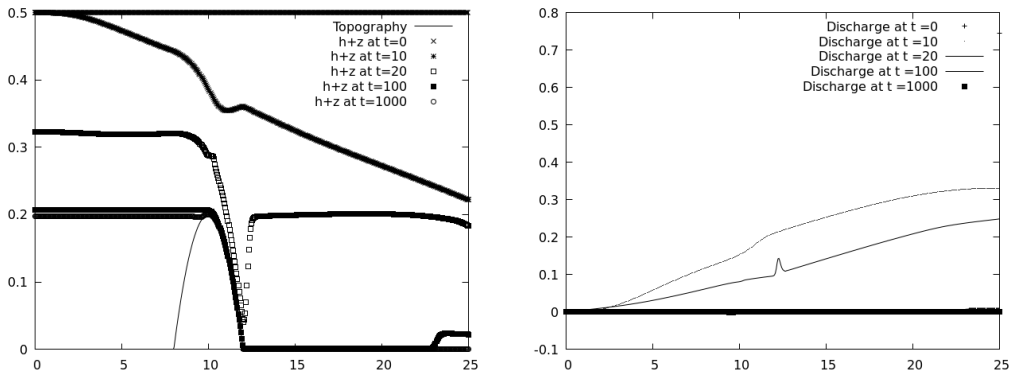

(a) (b)

Figure 14: Free surface (14a) and discharge (14b) for the simulation of drain on a non-flat bottom

while the right boundary condition is imposed as follows:

$$h_R = \min\left(\frac{1}{9g}(u_N^n + 2\sqrt{gh_N^n})^2, h_N^n\right) \qquad \text{and} \qquad q_R = \frac{h_R}{3}(u_N^n + 2\sqrt{gh_N^n}).$$

The domain discretization is made of 500 cells. In Figure 14, we displays the numerical approximation obtained at time $t_{end} = 0,\ 10,\ 20,\ 100,\ 1000$. Once again, we notice a very good behavior of the approximate solution.

Acknowledgements

Christophe Berthon and Meissa M'baye thank the ANR project MUFFIN ANR-19-CE46-0004 for financial supports.

References

[1] E. Audusse, F. Bouchut, M.-O. Bristeau, R. Klein, and B. Perthame. A fast and stable well-balanced scheme with hydrostatic reconstruction for shallow water flows. *SIAM Journal on Scientific Computing*, 25(6):2050–2065, 2004.

[2] A. Bermudez and M. E. Vazquez. Upwind methods for hyperbolic conservation laws with source terms. *Computers & Fluids*, 23(8):1049–1071, 1994.

[3] C. Berthon and C. Chalons. A fully well-balanced, positive and entropy-satisfying godunov-type method for the shallow-water equations. *Mathematics of Computation*, 85(299):1281–1307, 2016.

[4] C. Berthon, A. Crestetto, and F. Foucher. A well-balanced finite volume scheme for a mixed hyperbolic/parabolic system to model chemotaxis. *Journal of Scientific Computing*, 67(2):618–643, 2016.

[5] C. Berthon and F. Marche. A positive preserving high order VFRoe scheme for shallow water equations: a class of relaxation schemes. *SIAM J. Sci. Comput.*, 30(5):2587–2612, 2008.

[6] F. Bouchut. *Nonlinear stability of finite volume methods for hyperbolic conservation laws and well-balanced schemes for sources*. Frontiers in Mathematics. Birkhäuser Verlag, Basel, 2004.

[7] M. Castro, J. Gallardo, and C. Parés. High order finite volume schemes based on reconstruction of states for solving hyperbolic systems with nonconservative products. Applications to shallow-water systems. *Mathematics of computation*, 75(255):1103–1134, 2006.

[8] M. J. Castro, A. Pardo Milanés, and C. Parés. Well-balanced numerical schemes based on a generalized hydrostatic reconstruction technique. *Mathematical Models and Methods in Applied Sciences*, 17(12):2055–2113, 2007.

[9] G. Chen and S. Noelle. A new hydrostatic reconstruction scheme based on subcell reconstructions. *SIAM Journal on Numerical Analysis*, 55(2):758–784, 2017.

[10] O. Delestre, S. Cordier, F. Darboux, and F. James. A limitation of the hydrostatic reconstruction technique for shallow water equations. *C. R. Math. Acad. Sci. Paris*, 350(13-14):677–681, 2012.

[11] G. Gallice. Schémas de type godunov entropiques et positifs pour la dynamique des gaz et la magnétohydrodynamique lagrangiennes. *Comptes Rendus de l'Académie des Sciences-Series I-Mathematics*, 332(11):1037–1040, 2001.

[12] G. Gallice. Positive and entropy stable godunov-type schemes for gas dynamics and mhd equations in lagrangian or eulerian coordinates. *Numerische Mathematik*, 94(4):673–713, 2003.

[13] T. Gallouët, J.-M. Hérard, and N. Seguin. Some approximate godunov schemes to compute shallow-water equations with topography. *Computers & Fluids*, 32(4):479–513, 2003.

[14] E. Godlewski and P.-A. Raviart. *Numerical approximation of hyperbolic systems of conservation laws*, volume 118 of *Applied Mathematical Sciences*. Springer-Verlag, New York, 1996.

[15] S. K. Godunov. A difference method for numerical calculation of discontinuous solutions of the equations of hydrodynamics. *Mat. Sb. (N.S.)*, 47(89):271–306, 1959.

[16] L. Gosse. A well-balanced flux-vector splitting scheme designed for hyperbolic systems of conservation laws with source terms. *Computers & Mathematics with Applications*, 39(9):135–159, 2000.

[17] N. Goutal and F. Maurel. Dam-break wave simulation. In *Proceedings of the First CADAM workshop*, 1998.

[18] J. M Greenberg and A.-Y. Leroux. A well-balanced scheme for the numerical processing of source terms in hyperbolic equations. *SIAM Journal on Numerical Analysis*, 33(1):1–16, 1996.

[19] J. M. Greenberg, A. Y. Leroux, R. Baraille, and A. Noussair. Analysis and approximation of conservation laws with source terms. *SIAM Journal on Numerical Analysis*, 34(5):1980–2007, 1997.

[20] A. Harten, P.D. Lax, and B. Van Leer. On upstream differencing and Godunov-type schemes for hyperbolic conservation laws. *SIAM review*, 25:35–61, 1983.

[21] S. Jin. A steady-state capturing method for hyperbolic systems with geometrical source terms. *ESAIM: Mathematical Modelling and Numerical Analysis*, 35(04):631–645, 2001.

[22] V. Michel-Dansac, C. Berthon, S. Clain, and F. Foucher. A well-balanced scheme for the shallow-water equations with topography. *Computers & Mathematics with Applications*, 72(3):568–593, 2016.

[23] V. Michel-Dansac, C. Berthon, S. Clain, and F. Foucher. A well-balanced scheme for the shallow-water equations with topography or manning friction. *Journal of Computational Physics*, 335:115–154, 2017.

[24] S. Noelle, Y. Xing, and C.-W. Shu. High-order well-balanced finite volume WENO schemes for shallow water equation with moving water. *J. Comput. Phys.*, 226(1):29–58, 2007.

[25] G. Russo and A. Khe. High order well balanced schemes for systems of balance laws. In *Hyperbolic problems: theory, numerics and applications*, volume 67 of *Proc. Sympos. Appl. Math.*, pages 919–928. Amer. Math. Soc., Providence, RI, 2009.

[26] G. Russo and A. Khe. High order well-balanced schemes based on numerical reconstruction of the equilibrium variables. In *Proceedings "WASCOM 2009" 15th Conference on Waves and Stability in Continuous Media*, pages 230–241. World Sci. Publ., Hackensack, NJ, 2010.

[27] D. Serre. *Systems of conservation laws. 1.* Cambridge University Press, Cambridge, 1999. Hyperbolicity, entropies, shock waves, Translated from the 1996 French original by I. N. Sneddon.

[28] E. F. Toro. *Riemann solvers and numerical methods for fluid dynamics.* Springer-Verlag, Berlin, third edition, 2009. A practical introduction.

[29] E.F. Toro, M. Spruce, and W. Speares. Restoration of the contact surface in the HLL-Riemann solver. *Shock waves*, 4(1):25–34, 1994.

[30] Y. Xing. Exactly well-balanced discontinuous Galerkin methods for the shallow water equations with moving water equilibrium. *J. Comput. Phys.*, 257(part A):536–553, 2014.

[31] Y. Xing, C.-W. Shu, and S. Noelle. On the advantage of well-balanced schemes for moving-water equilibria of the shallow water equations. *Journal of Scientific Computing*, 48(1-3):339–349, 2011.